International Journal of Current Science, Engineering & Technology ISSN : 2581-4311
Original Research Article| Open Access

In Effect of reducing agents in the preparation and light harvesting properties of $CuInS_2$ nanoparticles

Rajitha Beerelli[a,b], Niveditha Reddy Barray[c], Satish Bykkam[c], Venkateswara Rao Kalagadda[c], Padma Suvarna R[a]*

[a]Department of Physics, Jawaharlal Nehru Technological University Ananthapur, Ananthapur, Andhra Pradesh, India.

[a]Department of Physics, BVRIT Hyderabad College of Engineering for Women, JNTUH, Hyderabad, Telangana State, India.

[b]Centre for Nanoscience and Technology, Institute of Science and Technology, Jawaharlal Nehru Technological University Hyderabad, Hyderabad, Telangana State, India.

Received: 28 December 2017; **Revised:** 04 February 2018; **Accepted:** 07 February 2018; **Published online:** 11 February 2018;

ABSTRACT: Tetragonal Copper Indium disulphide ($CuInS_2$) nanoparticles in the size range of 80 nm were prepared by microwave assisted solution synthesis process. Three different Sulphur sources namely, thioacetamide (TAA), thiourea and l-cysteine were used in this process. In this regard, samples showed no evident difference in their morphological or structural properties when prepared by all through all three sources. Accordingly the band gap of all the samples remained close 2.2 eV and did not deviate much. However solar cell tests and photocatalytic degradation studies revealed the advantage of thiourea as a Sulphur source over its counterparts. A form factor (FF) of 34% and 73% degradation efficiency of methyl orange were shown by $CuInS_2$ nanoparticles prepared by thiourea as opposed to 30% FF in other samples.

Keywords: *$CuInS_2$ nanoparticles; Thiourea;Photocatalytic degradation; Degradation efficiency;*

1. INTRODUCTION

Copper Indium Sulphide ($CuInS_2$) is a cheaper non-toxic alternative of its copper indium selenide ($CuInSe_2$) compound semiconductor counterpart [1]. Both these materials have appealed the attention of renewable energy scientists who were fascinated by the theoretical efficiency (30%) of solar cells constructed using these materials [2]. However, the maximum achieved efficiency till date has only been 15%. In this regard, multiple synthesis techniques which modify the physio-chemical properties of $CuInS_2$ have been tried and tested in the past. However, seldom these processes have resulted in any observable difference in the efficiency of the solar cells [3].

Various methods have been used in the preparation of $CuInS_2$ nanoparticles and thinfilms. Some of the most notable methods include electrodeposition [4], wet chemical methods [5,6], solution combustion synthesis [7], spray pyrolysis[8], electroplated precursors [9], ion layer gas reaction method [10] etc. Of these methods, wet chemical methods for the preparation of $CuInS_2$ nanoparticles and thin films subsequently remain the most economical and efficient [11, 12]. In this regard, multiple methods including co-precipitation [13, 14], sol-gel synthesis [15] and microwave synthesis [16-17] have remained to be the most popular. Among these methods, microwave synthesis stands apart as the easiest, for the preparation of nanoparticles. Accordingly many nanoparticles including CuInS2 nanoparticles have been prepared via this method [18-21]. It has been observed that usage of different pre-cursors result in the formation of various morphological and structural properties for nanoparticles. In this regard, nanoparticles of $CuInS_2$ have been prepared using multiple Sulphur sources such as thioacetamide (TAA),thiourea and l-cysteine in the past [22]. However, limited reports have shown the difference between nanoparticles prepared by these sources. In this paper, we report the preparation of $CuInS_2$ nanoparticles using afore mentioned three Sulphur sources via microwave synthesis process. Furthermore their morphology, structural properties, solar cell efficiency and photocatalytic degradation of methyl orange have been studied extensively and a consolidated report of the same has been generated.

2. MATERIALS AND METHODS

All the chemicals used in this study, if mentioned otherwise, were procured from Sigma Aldrich, USA and were used without further purification. Distilled water and propylene glycol were used as solvents in all the reactions.

Correspondence
R. Padma Suvarna; padmajntua@gmail.com

DOI: *10.30967/ijcrset.1.1.2018.24-29*

Competing interests
The authors have declared that no competing interests exist.

Cite this article
Rajitha, B., Nideditha Reddy, B., Satish, B., Venkateswara Rao, K., & Padma Suvarna, R. (2018). In Effect of reducing agents in the preparation and light harvesting properties of $CuInS_2$ nanoparticles.*Int J Cur Res EngSci Tech. 1(1): 24-29.*

2.1 Synthesis of $CuInS_2$ nanoparticles

In a typical synthesis method, $Cu(SO_4)_2.H_2O$, $InCl_3$ anhydrous and different sulfur sources (thioacetamide (TAA), thiourea or l-cysteine) were weighed in a molar ratio of 1:1:2 and dissolved in 30 ml propylene glycol along with Sodium dodecyl sulfate (SDS) as a capping agent. The precursor solutions were sintered in a microwave muffle furnace (CEM, USA, PHOENIX AIRWAVE) and cooled naturally to room temperature in ambient air conditions. Post stirring, a black precipitate was produced, which was filtered, washed with distilled water, and then dried at 80 °C for 4 h.

2.2 Characterization

X-ray diffraction (XRD, Philips-X'PertPro) was performed using Ni-filtered Cu Kα radiation between 2θ values of 10 and 80. Scanning electron microscopy (SEM) images were obtained on a LEO-1455VP equipped with an energy dispersive X-ray spectrometer (XL30, Philips microscope). The room temperature photoluminescence (PL) properties were studied on a Perkin-Elmer (LS 55) fluorescence spectrophotometer. Band gap of the nanoparticles were obtained through Scinco UV-vis scanning spectrometer (Model S-10 4100). The Fourier transform infrared (FT-IR, Magna Nicolet 550) spectrum was recorded using KBr pellets.

2.3 Photocatalytic Degradation

Photocatalytic degradation studies were conducted on all the samples using methyl orange as the model contaminant. Briefly, 0.5 mg of methyl orange was mixed with $CuInS_2$ nanoparticles (5 mg/mL) in 50 mL of distilled water. The samples were aged for 270 minutes in a dark chamber in order to reach adsorption equilibrium before they were placed inside the photo-reactor for degradation studies. The samples were placed 15 cm from a 400 W Tungsten lamp for a brief period while multiple aliquot readings were taken at different time points to estimate methyl orange degradation via photocatalysis. Percentage degradation of methyl orange was calculated using the following formula.

$$\text{Degradation rate } (\%) = \frac{A_0 - A}{A_0} X100$$

Where A_0 and A are the absorbance of solution at A_0 and A min, respectively.

2.4 Solar Cell efficiency

The solar cell using $CuInS_2$ nanoparticles as the absorber layer was constructed in a similar fashion to earlier mentioned reports [23]. Briefly, slurries of $CuInS_2$ nanoparticles (0.05 gof nanoparticles, 0.05 g ofethyl cellulose and 0.05 mL of Triton X-100 in 5 mL of ethanol) were used to form p-type semiconducting layers via Doctor's blade method on Indium Tin oxide (ITO) substrate.

This was followed by the formation of CdS n-type semiconducting layer on ITO substrate via chemical bath deposition ($Cd(NO_3)_2$ (30 mL, 0.01 M) andthiourea (10 mL, 0.08 M) at 80°C). A platinum coated ITO was placed on top to complete the solar cell. The current density-voltage (J-V) characteristics of the fabricated CIS were measured under simulated illumination with a light intensity of 100 mW/cm^2 (AM 1.5).

3. RESULTS & DISCUSSION

3.1 Structural Analysis

The structural features for all the samples were studied using XRD. From figure 1, it is evident that all the samples formed tetragonal structures pertaining to JCPDS#38–0777. The peaks pertaining to thioureaand l-cystine appear broader than the ones obtained for thioacetamide. This could be due to the formation of smaller crystallites in the aforementioned samples. In order understand the same, crystallite sizes were determined using Debye Scherer's formula and results were 45, 35, and 30 nm for thioacetamide, thiourea and l-cysteine respectively. It is clear from these results that thiourea and l-cysteine reduce crystallite size of $CuInS_2$ nanoparticles even when used in the same molar concentration.

3.2 Morphology and Elemental Analysis

The effect of the sulfide on the morphology of the $CuInS_2$ nanostructures prepared using a microwave-assisted co-precipitation method was investigated by SEM. Figure. 2a, 2b, and 2c present SEM images of the nanoparticles formed from thioacetamide, thiourea, and l-cysteine, respectively. According to Figure 2a, the morphology of the sample was spherical, composed of a large number ofnanoparticles with a mean size of approximately80 nm. It is interesting to note that theeffectof these particular Sulphur sources have been recordedearlier by Hosseinpour-Mashkani et al [23]. The conclusion from the article shows that the slower nucleation

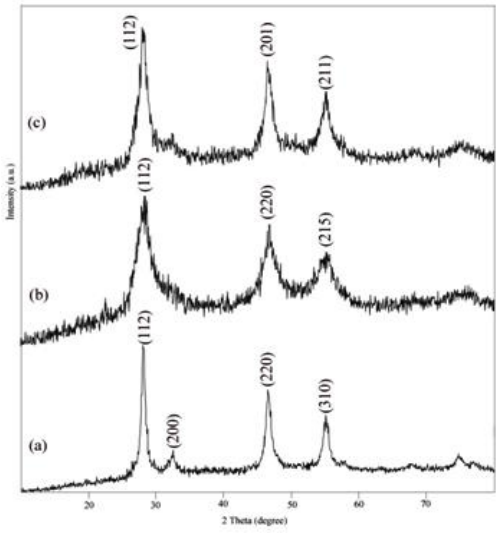

Fig. 1: XRD patterns of CuInS2 nanoparticles (a) TAA (b) thiourea (c) l-cystine

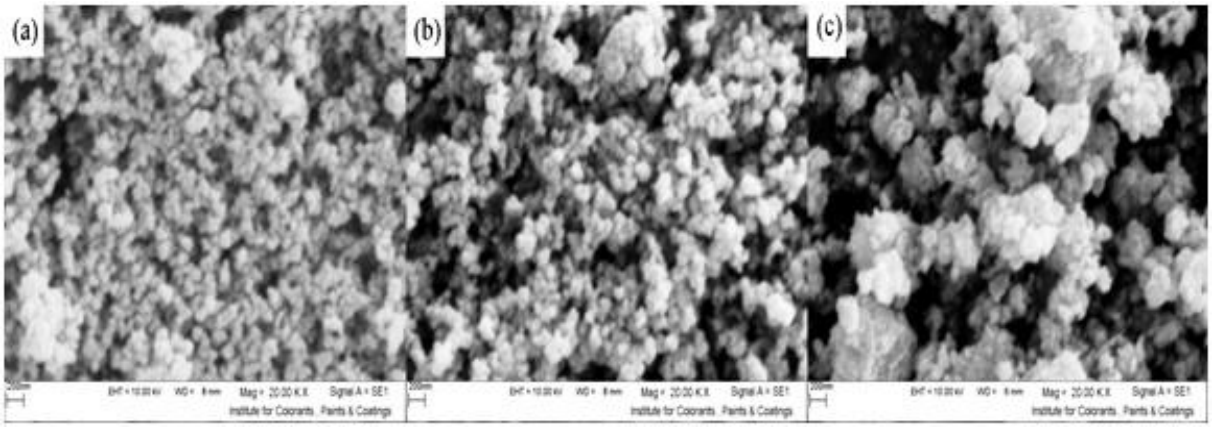

Fig.2: SEM images $CuInS_2$ nanoparticles (a) TAA (b) thiourea (c) l-cystine

of various Sulphur sources results in the formation of nanoparticles in different sizes. Although our synthesis procedure followed their procedure closely, we obtained a comparatively larger particle size of 80 nm as opposed 25-35 nm in theirs. It is also interesting to note that the particle sizes of the nanoparticles that were prepared by thiourea were comparatively smaller (80 nm) than those prepared by thioacetamide and l-cysteine (120 nm and 150 nm respectively). As mentioned above this could be due to the slower dissociation of thiourea as opposed to its counterparts during the formation of $CuInS_2$ nanostructures.

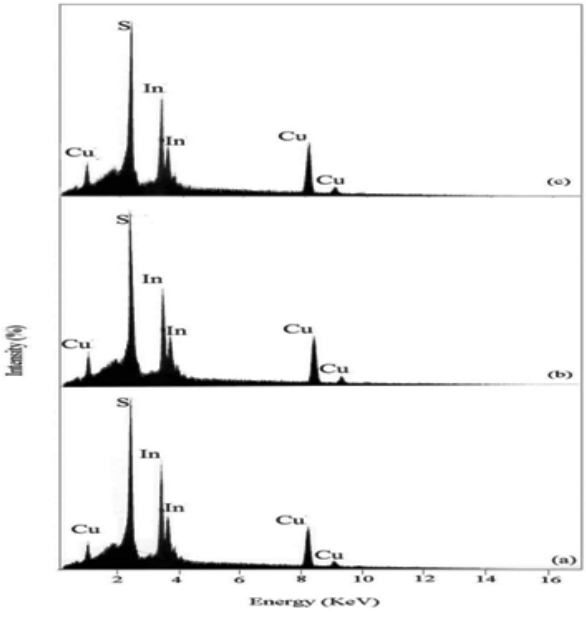

Fig. 2: EDS pattern of $CuInS_2$ nanoparticles (a) TAA (b) thiourea (c) l-cystine

Elemental analysis of the samples was conducted to understand the purity of the sample. Figure. 3a, b, and c present the EDS data of $CuInS_2$nanoparticles synthesized in the presence of thioacetamide, thiourea, and l-cysteine as the Sulphur sources respectively. As shown in Fig. 3a, b, & c present the EDS data of $CuInS_2$nanoparticles synthesized in the presence of thioacetamide, thiourea, and l-cysteine as the Sulphur sources respectively. In Fig. 3(a-c) Cu, In, and S were observed and in addition, neither N nor C signals were detected in the EDS spectrum, which indicate the absence of residual surfactant or solvent in the nanoparticles.

3.3 Photoluminescent Spectra:

The photoluminescence (PL) spectra of the $CuInS_2$ nanoparticles obtained from thioacetamide, thiourea, and l-cysteine recorded in ethanol and are seen in figure 4 a, b and c respectively. The emission peaks at 544.5, 568.6, and 418 nm were observed for thioacetamide, thiourea, and l-cysteine samples respectively which correspond to a band gap of 2.27, 2.26, and 2.96 eV, respectively. These values are greater than those observed for bulk $CuInS_2$(1.4 to 1.5 eV) which could be attributed to the blue shift due to the decrease in their particle size. However such high increase in the band gap has been observed for the first time. Although previously these anomalies were attributed todefective crystal formation, we proposethat this could be due to the phenomenal decrease in the crystallite size as opposed to particle size of $CuInS_2$.

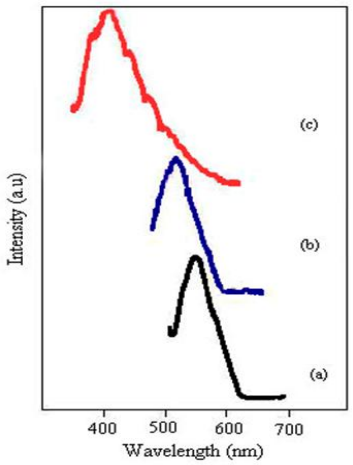

Fig. 4: Room temperature PL spectra of $CuInS_2$ nanoparticles (a) TAA (b) thiourea (c) l-cystine

3.4 Photocatalytic degradation of Methyl Orange

The photocatalytic properties of the $CuInS_2$ nanoparticles prepared by thioacetamide as Sulphur source was tested using methyl orange as the model effluent. Only these set of nanoparticles were chosen based on the PL result which indicated the most desired band gap for nanoparticles prepared by thioacetamide. The results are shown in figure 5a and 5b where it is clearly evident that the nanoparticles show no activity in the absence of light while reduce methyl orange efficiently in the presence of visible light. Furthermore, the UV spectral result measured at various time points (post light exposure) indicate a steady decrease in the methyl orange concentration with increasing time.

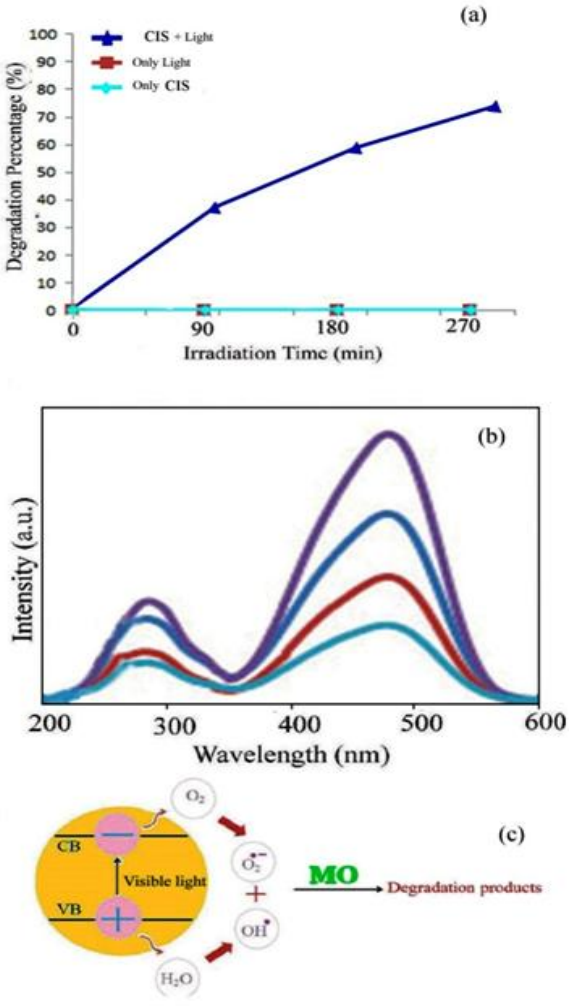

Fig. 5(a): photocatalytic methyl orange degradation of CIS nanoparticles obtained from TAA as a sulfide source under visible light, (b)fluorescence spectral time scan of methyl orange illuminated at 365 nm with CIS nanoparticles, and (c) reaction mechanism of methyl orange photo degradation over CIS under visible light irradiation.

Finally the mechanism of action has been explained in figure 5c, where we presume that surface superoxide generated in the presence of visible light results in the effective degradation of methyl orange resulting in a single water molecule asrepresented below

$CIS + h\nu \rightarrow CIS^{\bullet} + e^{-} + h^{+}$ (1)

$h^{+} + H_2O \rightarrow OH^{\bullet}$ (2)

$e^{-} + O_2 \rightarrow O_2^{\bullet-}$ (3)

$OH^{\bullet} + O_2^{\bullet-}$ + methyl orange → Degradation products

The efficiency of degradation at the end of 270 min irradiation was calculated based on initial and finalconcentration of methyl orange in solution as 73%. Such high degradation efficiency can be attributed to the absorbent type of porous structure of CuInS2nanoparticles. Furthermore, the decrease in the particle size also correlates to the increase in surface are per volume leading to a greater adherent/absorptive property of these nanoparticles.

3.5 Solar Cell Studies

Light harvesting studies on different samples (absorber layer on a solar cell) were conducted by exposing themtoan artificial light source 100 mW/cm^2. The J-V curves

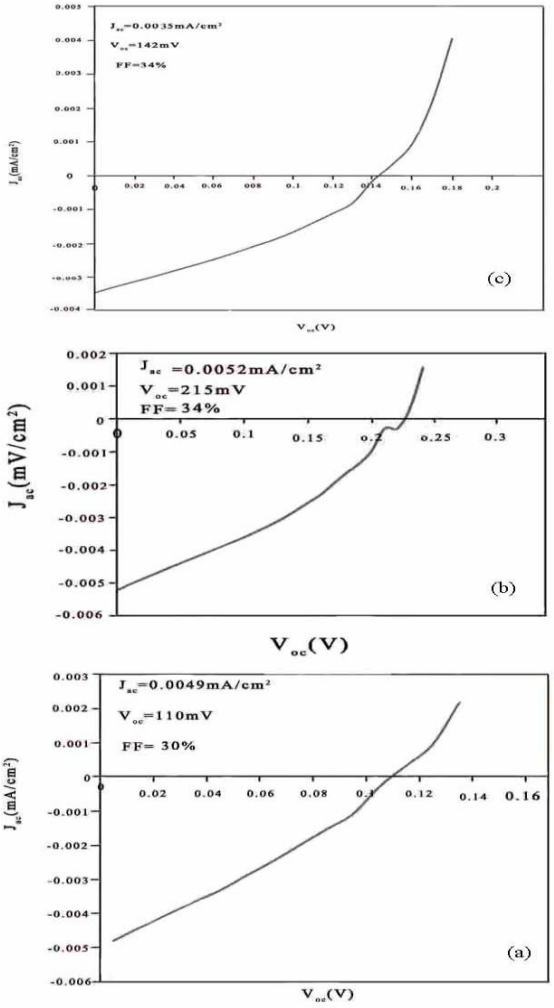

Fig. 6: I-V characterization of the ITO/CIS/CdS/Pt-ITO solar cell for (a) TAA (b) thiourea (c) l-cystine.

obtained for thiocetamide, thiourea and l-cysteine samples are presented in figure 6 a, b andcrespectively and the device characteristics for the same are: Voc =110 mV, Jsc =0.0049 mA/cm^2, and FF=30%for TAA; Voc =215 mV, Jsc =0.0052 mA/cm^2, and FF=34% for thiourea; and Voc =142 mV, Jsc =0.0035 mA/cm^2, and FF=34% for l-cysteine**.** These results indicate a decrease in the FF and corresponding values showing that the constructed solar cells have lower efficiency as opposed to those prepared using bulk particles. Similar results have been reported earlier quoting defect formation and increase in band gap of $CuInS_2$nanoparticles which could have resulted in decreased light harvesting applications [23]. As opposed to popular belief, the reduction in particle size does not result in increased light absorption and greater solar cell efficiency.

4. CONCLUSIONS

$CuInS_2$ nanoparticles were synthesized by a microwave-assisted co-precipitation method and their photoluminescence and photovoltaic solar cell properties were investigated.their photoluminescence and photovoltaic solar cell properties were investigated. This study scrutinized the influence of the Sulphur sources on the morphology, photocatalytic and photovoltaic solar cell properties. Spherical shaped particles in the size range of 80 to 120 nm were prepared using the aforementioned method. In the presence of $CuInS_2$ nanoparticles (prepared by thioacetamide as Sulphur source) as a photocatalyst, the percentage of methyl orange degradation was approximately 73 % after 270 min irradiation with visible light. The preliminary result of the solar cell constructed using $CuInS_2$ nanoparticles as the absorber layer revealed the possibility of developing inexpensive solar cells. While J-V curves showed greater efficiency for the nanoparticles prepared using thiourea as the Sulphur source, it was clearly evident that the reduction in particle size could greatly decrease the light trapping efficiency due to defect formation and resulting low short-circuit current.

ACKNOWLEDGMENT

The author wish to acknowledge the Department of Centre for Nano Science and Technology (CNST), Institute of Science and Technology, Jawaharlal Nehru Technological University, Hyderabad and BVRIT Hyderabad College of Engineering for Women, Hyderabad, India for providing Lab Facilities and research encouragement.

REFERENCES

[1] Klenk, R., Klaer, J., Scheer, R., Lux-Steiner, M. C., Luck, I., Meyer, N., &Rühle, U. (2005). Solar cells based on CuInS2—an overview. *Thin Solid Films*, *480*, 509-514.

[2] Oikkonen, L. E., Ganchenkova, M. G., Seitsonen, A. P., &Nieminen, R. M. (2011). Vacancies in CuInSe2: new insights from hybrid-functional calculations. *Journal of Physics: Condensed Matter*, *23*(42), 422202.

[3] Liqiang, J., Xiaojun, S., Jing, S., Weimin, C., Zili, X., Yaoguo, D., &Honggang, F. (2003). Review of surface photovoltage spectra of nano-sized semiconductor and its applications in heterogeneous photocatalysis. *Solar Energy Materials and Solar Cells*, *79*(2), 133-151.

[4] Wijesundera, R. P., &Siripala, W. (2004). Preparation of CuInS2 thin films by electrodeposition and sulphurisation for applications in solar cells. *Solar energy materials and solar cells*, *81*(2), 147-154.

[5] Bourlier, Y., Bernard, R., Lethien, C., Roussel, P., Zegaoui, M., Bouazaoui, M., ...& Rolland, P. A. (2012). Hall-Effect Measurements of Sol–Gel Derived CuInS2 Thin Films for Photovoltaic Applications. *Applied Physics Express*, *5*(12), 125801.

[6] Hou, X., & Choy, K. L. (2005). Synthesis and characteristics of CuInS2 films for photovoltaic application. *Thin Solid Films*, *480*, 13-18.

[7] Wakita, K., Iwai, M., Miyoshi, Y., Fujibuchi, H., &Ashida, A. (2005). Synthesis of CuInS2 nanowires and their characterization. *Composites science and technology*, *65*(5), 765-767.

[8] Ryo, T., Nguyen, D. C., Nakagiri, M., Toyoda, N., Matsuyoshi, H., & Ito, S. (2011). Characterization of superstrate type CuInS2 solar cells deposited by spray pyrolysis method. *Thin Solid Films*, *519*(21), 7184-7188.

[9] Onuma, Y., Takeuchi, K., Ichikawa, S., Suzuki, Y., Fukasawa, R., Matono, D., & Ito, K. (2003). Cross-sectional analysis of CuInS2 thin film prepared from electroplated precursor. *Japanese journal of applied physics*, *43*(1A), L108.

[10] Qiu, J., Jin, Z., Wu, W., & Xiao, L. X. (2006). Characterization of CuInS2 thin films prepared by ion layer gas reaction method. *Thin Solid Films*, *510*(1-2), 1-5.

[11] Deng, W., Yan, Z., Fang, Y., & Wang, Y. (2014). Effect of Al content on the performance of Cu (In 1− x Al x) S 2 synthesized by hydrothermal solution processing. *Journal of Materials Science: Materials in Electronics*, *25*(6), 2829-2834.

[12] Gusain, M., Kumar, P., &Nagarajan, R. (2013). WurtziteCuInS 2: solution based one pot direct synthesis and its doping studies with non-magnetic Ga 3+ and magnetic Fe 3+ ions. *RSC Advances*, *3*(41), 18863-18871.

[13] Jung, S., Cha, J. H., & Jung, D. Y. (2016). Synthesis of oleic acid-capped CuInS2 nanocrystals from bimetallic hydroxide precursor. *Thin Solid Films*, *603*, 243-248.

[14] Song, W. S., & Yang, H. (2013). Solvothermal preparation of yellow-emitting CuInS2/ZnS quantum dots and their application to white light-emitting diodes. *Journal of nanoscience and nanotechnology*, *13*(9), 6459-6462.

[15] Mange, Y. J., Dewi, M. R., Macdonald, T. J., Skinner, W. M., &Nann, T. (2015). Rapid microwave assisted synthesis of nearly monodisperse aqueous CuInS 2/ZnS nanocrystals. *CrystEngComm*, *17*(41), 7820-7823.

[16] Krylova, G., Yashan, H., Hauck, J. G., Burns, P. C., McGinn, P. J., & Na, C. (2015). Microwave-Assisted Solution–Liquid–Solid Synthesis of Single-Crystal Copper Indium Sulfide Nanowires. *Crystal Growth & Design*, *15*(6), 2859-2866.

[17] Sabet, M., Salavati-Niasari, M., Ghanbari, D., Amiri, O., &Yousefi, M. (2013). Synthesis of CuInS2 nanoparticles via simple microwave approach and investigation of their behavior in solar cell. *Materials Science in Semiconductor Processing, 16*(3), 696-704.

[18] Salavati-Niasari, M., Hosseinpour-Mashkani, S. M., &Mohandes, F. (2015). Effect of precursor, microwave power and irradiation time on the particle size of CuInS 2 nanoparticles. *Journal of Materials Science: Materials in Electronics, 26*(10), 7936-7947.

[19] Susaki, M. (2005). Rapid preparation of CuInS2 bulk polycrystals by two-step microwave heating process using a domestic microwave oven. *Japanese journal of applied physics, 44*(6L), L866.

[20] Wang, Y., Zhao, X., Liu, F., Zhang, X., Chen, H., Bao, F., & Liu, X. (2014). Selective synthesis of cubic and hexagonal phase of CuInS 2 nanocrystals by microwave irradiation. *RSC Advances, 4*(31), 16022-16026.

[21] Zhang, J., Chen, J., & Li, Q. (2015). Microwave heating synthesis and formation mechanism of chalcopyrite structured CuInS2 nanorods in deep eutectic solvent. *Materials Research Bulletin, 63*, 88-92.

[22] Hosseinpour-Mashkani, S. M., Salavati-Niasari, M., &Mohandes, F. (2014). CuInS2 nanostructures: synthesis, characterization, formation mechanism and solar cell applications. *Journal of Industrial and Engineering Chemistry, 20*(5), 3800-3807.

[23] Ostrovskii, I., &Cremaldi, L. (2012). Resonances in ferroelectric phononicsuperlattice. *Applied Physics Letters, 101*(15), 152902.